Draft version April 6, 2026
Typeset using LaTeX **twocolumn** style in AASTeX7.0.1

Extreme Values of Black Hole to Stellar Mass Ratio for High-Redshift Galaxies

Cameron Heather,[1] Teeraparb Chantavat,[2] Siri Chongchitnan,[1] and Josesph Silk[3,4]

[1] Warwick Mathematics Institute, University of Warwick, Zeeman Building, Coventry CV4 7AL, UK
[2] Institute for Fundamental Study, Naresuan University, Phitsanulok, 65000, Thailand
[3] Institut d'Astrophysique de Paris, 98 bis Boulevard Arago, 75014, Paris, France
[4] William H. Miller III Department of Physics and Astronomy,The Johns Hopkins University, Baltimore, MD 21218, USA

ABSTRACT

With recent data from the *James Webb Space Telescope* (JWST), it is possible to calculate the mass of the supermassive black holes at the centre of galaxies, and the stellar mass of the host galaxies at $z \gtrsim 5$. In this work, we apply the method of extreme-value statistics to calculate the distributions of extreme black hole and stellar mass for the redshift range $3.5 \lesssim z \lesssim 8.5$. We sample these distributions to obtain a prediction for the black hole to stellar mass ratio of ~ 0.24 over this redshift range, with the median in each bin varying in the range $0.18 - 0.35$. Our predictions are consistent with the highest observed values of the ratio from JWST observations of high-redshift galaxies.

1. INTRODUCTION

The *James Webb Space Telescope* (JWST) has now revealed hundreds of galaxies at redshift $z \gtrsim 5$, shedding new light on galaxy evolution in the Universe less than a billion years after the Big Bang (e.g., S. L. Finkelstein et al. (2023); R. P. Naidu et al. (2022)). Using JWST NIRSpec/NIRCam instruments, supermassive black holes (SMBH) at the centre of these high-redshift galaxies can be probed, and their masses inferred from broad emission lines (e.g., Y. Harikane et al. (2023); R. Maiolino et al. (2024)). In addition, the stellar mass in these galaxies can be estimated by spectral energy distribution fitting of host galaxies, though with significant uncertainties due to dust and nebular emission.

These observations revealed that some high-redshift SMBHs are disproportionately massive with respect to their host galaxies. Recent JWST observations found M_{BH}/M_* as large as 10% for galaxies at $z \gtrsim 5$ (V. Kokorev et al. 2023; J. Matthee et al. 2025; M. Yue et al. 2024). This is in contrast to the much lower previously held pre-JWST values of $(M_{BH}/M_*) \sim 10^{-3}$ (N. Häring & H.-W. Rix 2004; L. Ferrarese & D. Merritt 2000; A. E. Reines & M. Volonteri 2015). Several ultra-high redshifts AGNs ($z > 10$) suggest that galaxies could even form with over-massive SMBH with $(M_{BH}/M_*) \sim 1$ (Á. Bogdán et al. 2024; F. Pacucci & A. Loeb 2024)

These high ratios challenge traditional models of how SMBHs and their host galaxies co-evolve, and raise questions about the physics of SMBH growth in the early Universe. A host of exotic physics have been proposed, such as super-Eddington accretion (E. Pezzulli et al. 2016), top-heavy initial mass functions (H. Haghi et al. 2020), and seeding by extreme Pop III stars (T. Chantavat et al. 2023). Nevertheless, a consistent theoretical framework has yet to emerge.

In this work, we demonstrate that extreme values of the ratio M_{BH}/M_* can be explained using the extreme-value statistics. By adopting empirical mass functions, we show that extreme ratios as high as 0.3 at redshift $z \sim 4-8$ can be expected without invoking exotic growth physics.

In Sec. 2, we describe the black hole and halo mass functions we use for our EVS application, both of which are fitted Schechter functions. In Sec. 3, we will introduce the extreme-value formalism from which we derive the extreme distributions of each of the mass functions. We use these distributions to calculate the black hole to stellar mass ratio $M_{\rm BH}/M_*$ in Sec. 4, comparing our findings with JWST data. Our conclusions and discussion are given in Sec. 5.

We will assume a flat ΛCDM cosmology with $H_0 = 70\text{km s}^{-1}\text{Mpc}^{-1}$, $\Omega_{\rm m} = 0.32$ and $\Omega_\Lambda = 0.68$.

2. BLACK HOLE AND STELLAR MASS FUNCTIONS

To calculate the distribution of the ratio $M_{\rm BH}/M_*$, we start with the black hole mass function and stellar mass function, where both are fitted using the Schechter

Email: cameron.heather@warwick.ac.uk

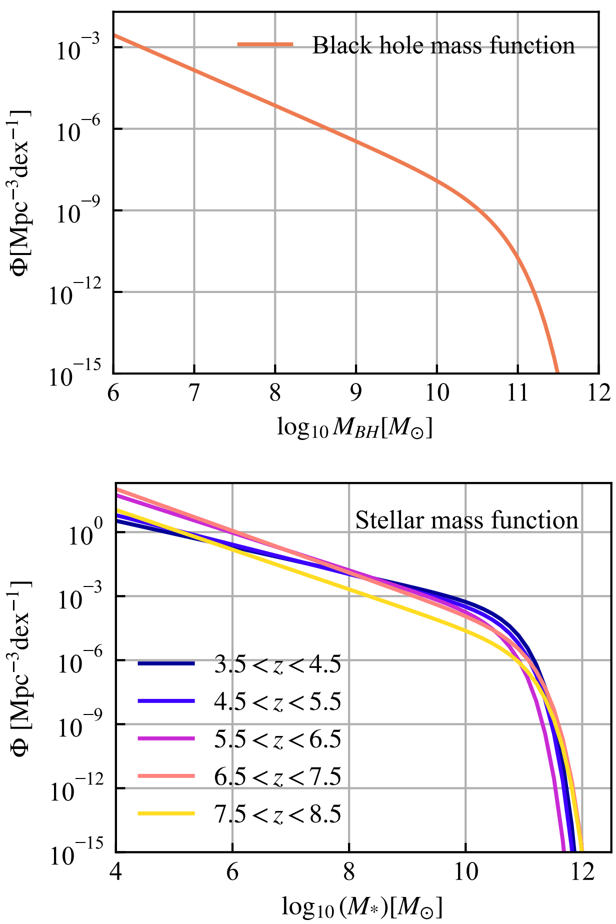

Figure 1. Plots of the black hole mass function (top) from (A. J. Taylor et al. 2025) and the stellar mass function (bottom) from R. Navarro-Carrera et al. (2024). The black hole mass function is given in a single redshift bin $z \sim 4-8$, whereas the stellar mass function is given in the binned redshift range $z = 3.5-8.5$. Both are Schechter functions of the form given in Eq. 1.

function (P. Schechter 1976) of the form

$$\Phi(M) \propto \left(\frac{M}{M_c}\right)^{1-\alpha} e^{-M/M_c}, \quad (1)$$

where α and M_c are empirically fitted parameters. These parameters for the black hole mass functions are given in A. J. Taylor et al. (2025), and the stellar mass parameters are given in R. Navarro-Carrera et al. (2024), where they are corrected for Eddington bias. We plot these mass functions in Fig. 1. The A. J. Taylor et al. (2025) function does not evolve in the redshift range $3.5 < z < 6$. We will extrapolate the black hole mass function to $z \sim 8$, effectively assuming that the most massive SMBHs were already in place by $z \sim 8$, so the tail of the mass function (and only the tail is important in our work) should not evolve significantly with redshift. The stellar mass function of R. Navarro-Carrera et al. (2024) also shows weak redshift dependence and a non-monotonic evolution over the redshift bins $[3.5, 4.5], [4.5, 5.5], [5.5, 6.5], [6.5, 7.5], [7.5, 8.5]$. We follow this binning in our work.

3. EXTREME-VALUE MODELLING

Our goal is to calculate the extreme distribution for both the black hole mass function and the stellar mass function, from which we can calculate the ratio by sampling these extreme distributions. This framework has previously been used to calculate the extreme halo and stellar mass for galaxies (C. C. Lovell et al. 2023), the most massive Pop III stars (T. Chantavat et al. 2023), primordial black holes (S. Chongchitnan et al. 2021; S. Chongchitnan & J. Silk 2021), and, more recently, the brightest galaxies and AGNs at high redshifts (C. Heather et al. 2024, 2025).

We will be working with the generalised extreme value (GEV) approach, also known as the block maxima method (E. J. Gumbel 1958). In this method, we divide the observational volume into into N distinct blocks. From this we identify the most massive galaxy in each block using a probability density function outlined below. This method is analogous to the Central Limit Theorem, where the most massive galaxies will have a large-N distribution which corresponds to one of the three possible GEV distributions.

We follow the same pipeline for both the BH mass function from A. J. Taylor et al. (2025) and the stellar mass function from R. Navarro-Carrera et al. (2024). This pipeline is outlined below.

First, we calculate the number count of galaxies with mass greater than M_{gal} in a given redshift bin using

$$n(> M_{gal}) = \int_{z_{\min}}^{z_{\max}} \int_{M_{gal}}^{\infty} \frac{\mathrm{d}n}{\mathrm{d}M'_{gal}}\ \mathrm{d}M'_{gal}\ \mathrm{d}z, \quad (2)$$

where M_{gal} is either black hole mass $M_{\rm BH}$ or stellar mass M_*.

Next, we calculate P_0, the probability that no galaxies in a given volume V will have black hole or stellar mass exceeding M_{gal}. We assume the observed sky fraction $f_{sky} = 1$, to obtain generic predictions on the extreme masses. The probability distribution $P_0(M_{gal})$ can be modelled as a Poisson distribution with the following cumulative distribution function (cdf),

$$P_0(M_{gal}) = \exp(-n(> M_{gal})V). \quad (3)$$

According to the GEV formalism, P_0 is well approximated in the large-N limit by the following so-called

GEV distribution:

$$G(M_{gal}) = \begin{cases} \exp\left(-(1+\gamma y)^{-1/\gamma}\right) & (\gamma \neq 0), \\ \exp\left(-e^{-\gamma}\right) & (\gamma = 0), \end{cases} \quad (4)$$

where $y = (M_{gal} - \alpha)/\beta$. The parameters α, β describe the location of the peak and the scale of the pdf, while the sign of γ determines which GEV distribution the pdf corresponds to. In particular, $\gamma = 0,\ \gamma > 0,\ \gamma < 0$ corresponds to the Gumbel, Fréchet and Weibull distributions, respectively. We can express these parameters in terms of M_{gal} and V by Taylor-expanding Eqs. (3) and (4) around the peak of the pdf M_{peak} to cubic order. We obtain:

$$\gamma = n(> M_{peak})V - 1$$

$$\beta = \frac{(1+\gamma)^{1+\gamma}}{\frac{\mathrm{d}n}{\mathrm{d}M_{gal}}|_{M_{peak}} M_{peak} V}$$

$$\alpha = M_{peak} - \frac{\beta}{\gamma}\left((1+\gamma)^{-\gamma} - 1\right)$$

For both the black hole and stellar mass functions, we found γ to be negative, and in particular $\gamma \in [-0.15, 0]$, meaning that the GEV distributions are well approximated by the Weibull distribution.

4. EVS PREDICTIONS FOR BLACK HOLE TO STELLAR MASS RATIO

To calculate the black hole to stellar mass ratio, we sample from both of our extreme distributions using the inverse Weibull distribution obtained from inverting Eq. (4).

We take 10^4 samples from the extreme distributions, from which we compute the median value of $M_{\rm BH}/M_*$ as well as the 99^{th} and 95^{th} percentiles. We plot these as confidence intervals in Fig. 2, which is the main result of this work. The median values of $M_{\rm BH}/M_*$ are given in Table 1, along with the 95% percentile. We found an average ratio value of ~ 0.24 across the full redshift range $z \sim 4-8$.

We note that the non-monotonicity of the EVS predictions across the bins stems from that in the stellar mass function of R. Navarro-Carrera et al. (2024). In particular, the characteristic mass in their fitted Schechter function evolves non-monotonically with redshift. A similar non-monotonic trend in the stellar mass function at high redshifts is also seen in J. R. Weaver et al. (2023).

Also in Fig. 2, we show the observed ratios from J. Matthee et al. (2025); M. Yue et al. (2024); V. Kokorev et al. (2023). We find these to be consistent (within the 95% percentile) with our calculated values.

The redshift bin $[5.5, 6.5]$ is interesting as the EVS prediction for the ratio is the highest amongst the bins,

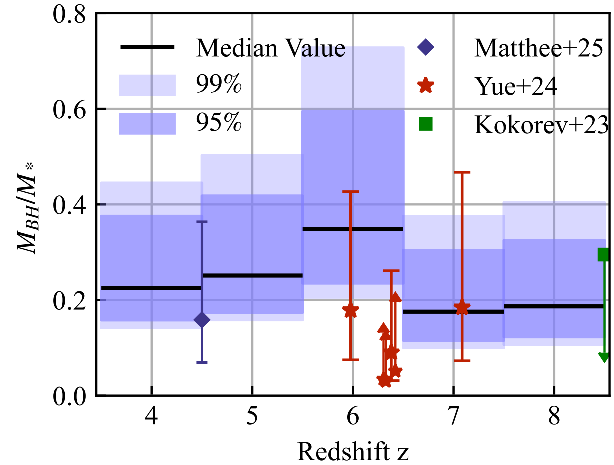

Figure 2. Plot of the EVS prediction for the extreme ratio M_{BH}/M_* for redshift bins in the range $z = 3.5 - 8.5$. The values for M_{BH} and M_* are calculated using the extreme-value modelling of the mass functions from A. J. Taylor et al. (2025) and R. Navarro-Carrera et al. (2024) respectively. The solid black line corresponds to the median, whilst the darker/lighter shaded area corresponds to the $95^{th}/99^{th}$ percentile. (See values in Table 1.) The data points are from J. Matthee et al. (2025); M. Yue et al. (2024); V. Kokorev et al. (2023), showing consistency with our EVS-derived estimates.

z	$[3.5, 4.5]$	$[4.5, 5.5]$	$[5.5, 6.5]$	$[6.5, 7.5]$	$[7.5, 8.5]$
$\frac{M_{\rm BH}}{M_*}$	$0.22^{+0.38}_{-0.14}$	$0.25^{+0.42}_{-0.16}$	$0.35^{+0.59}_{-0.21}$	$0.18^{+0.30}_{-0.10}$	$0.19^{+0.32}_{-0.11}$

Table 1. Predicted extreme values of the ratio M_{BH}/M_* in $z = 3.5-8.5$ (binned), plotted in Fig. 2. The 95th percentiles are also included.

and the observed ratio from M. Yue et al. (2024) shows a slight tension with our prediction. Focussing on this bin, we plot Fig. 3, which shows the black hole mass plotted against the stellar mass. Our EVS prediction is shown as an ellipse, and the dashed line shows a line with gradient $M_{\rm BH}/M_* = 0.35$ (the median EVS prediction). We see that observed data points from M. Yue et al. (2024) all lying below and to the mostly to the left of the ellipse as expected. We also deduce that the observed galaxy at $z \sim 11.5$ must have come from a galaxy with near extreme stellar mass, in contrast to the other data points in this bin.

5. DISCUSSION AND CONCLUSION

We have used extreme-value statistics to predict extreme-mass black hole and extreme stellar masses. The generalised extreme-value formalism shows that these extreme distributions are well approximated by Weibull distributions. We then sampled both distri-

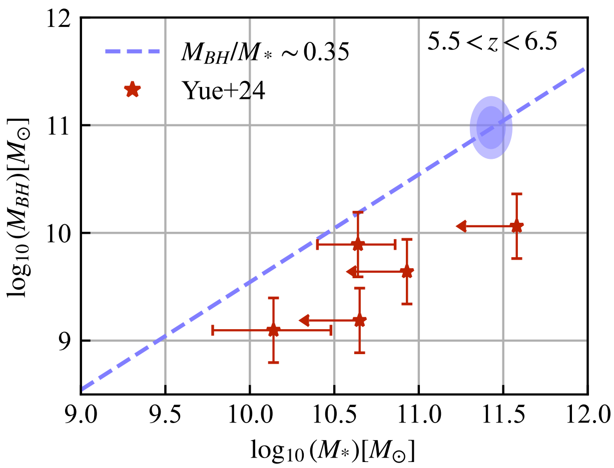

Figure 3. Plot of black hole mass against stellar mass. the blue dashed line corresponds to the calculated ratio $M_{\rm BH}/M_*$ for the redshift range $5.5 \lesssim z \lesssim 6.5$, where we plot the median value of $M_{\rm BH}/M_* \sim 0.35$. The ellipses show the distribution of the calculated extreme masses, providing an upper bound on both black hole and stellar mass. We include the data points from M. Yue et al. (2024) in this redshift range, along with their provided error bars.

butions and calculated the ratio $M_{\rm BH}/M_*$, provided in Table 1. In particular, we found the average value for this ratio across our whole redshift range to be $M_{\rm BH}/M_* \sim 0.24$. The distribution of this ratio against redshift is plotted in Fig. 2, and it is plotted again as a straight line in Fig. 3. The calculated values of $M_{\rm BH}/M_*$ using extreme-value statistics are in agreement with JWST observations from (V. Kokorev et al. 2023; J. Matthee et al. 2025; M. Yue et al. 2024; M. A. Stone et al. 2025).

In this work, we consider extreme black hole masses and extreme stellar masses. This hypothesis is supported by the observations shown in Fig. 3, where the extreme values of $M_{\rm BH}/M_*$ are associated with extreme galaxy stellar masses. In future work, we will explore the ratio $M_{\rm BH}/M_*$ for non-extreme black holes and stellar populations. A more nuanced approach to modelling the mass function would be required, for example, to establish a lower cut-off for the mass function to ensure convergence when the mass function is integrated.

Looking beyond $z \sim 8$, a quasar at $z \sim 10$ with $M_{\rm BH}/M_*$ as high as $M_{\rm BH}/M_* \sim 1$ was reported in Á. Bogdán et al. (2024). If confirmed, this exceeds the expected value of the ratio derived from the EVS formalism which only relies on the empirically fitted Schechter mass functions. A range of additional factors could modify these mass functions to drive up the EVS-derived ratio at higher redshifts, including a heavy black hole seed, bursts of super-Eddington accretion, and suppression of star formation with AGN feedback and duty cycle.

Equally, the EVS formalism could be used to calculate $M_{\rm BH}/M_*$ at lower redshifts ($z \sim 1$), where black holes and star formation couple more strongly through feedback-regulated co-evolution (J. Silk et al. 2024). However, this is limited by systematic uncertainties in black hole mass measurements. Applying our formalism to local and high-redshift galaxies would show how extreme-value statistics can trace regimes in which black hole growth and stellar assembly decouple, providing key insight into the physics of early galaxy formation.

ACKNOWLEDGEMENTS

Cameron Heather is supported by the Warwick Mathematics Institute Centre for Doctoral Training, and gratefully acknowledges funding from the University of Warwick and the UK Engineering and Physical Sciences Research Council (grant number: EP/W524645/1). This work was supported by Naresuan University (NU), and National Science, Research and Innovation Fund (NSRF). Grant NO.R2569B119.

DATA AVAILABILITY

The data used in this article will be shared on reasonable request to the corresponding author.

REFERENCES

Bogdán, Á., Goulding, A. D., Natarajan, P., et al. 2024, Nature Astronomy, 8, 126, doi: 10.1038/s41550-023-02111-9

Chantavat, T., Chongchitnan, S., & Silk, J. 2023, MNRAS, 522, 3256, doi: 10.1093/mnras/stad1196

Chongchitnan, S., Chantavat, T., & Zunder, J. 2021, Astronomische Nachrichten, 342, 648, doi: 10.1002/asna.202113826

Chongchitnan, S., & Silk, J. 2021, PhRvD, 104, 083018, doi: 10.1103/PhysRevD.104.083018

Ferrarese, L., & Merritt, D. 2000, ApJL, 539, L9, doi: 10.1086/312838

Finkelstein, S. L., Bagley, M. B., Ferguson, H. C., et al. 2023, ApJL, 946, L13, doi: 10.3847/2041-8213/acade4

Gumbel, E. J. 1958, Statistics of extremes (Columbia university press)

Haghi, H., Safaei, G., Zonoozi, A. H., & Kroupa, P. 2020, ApJ, 904, 43, doi: 10.3847/1538-4357/abbfb0

Harikane, Y., Ouchi, M., Oguri, M., et al. 2023, ApJS, 265, 5, doi: 10.3847/1538-4365/acaaa9

Häring, N., & Rix, H.-W. 2004, ApJL, 604, L89, doi: 10.1086/383567

Heather, C., Chantavat, T., Chongchitnan, S., & Chainakun, P. 2025, MNRAS, 543, 3783, doi: 10.1093/mnras/staf1690

Heather, C., Chantavat, T., Chongchitnan, S., & Silk, J. 2024, MNRAS, 534, 173, doi: 10.1093/mnras/stae2051

Kokorev, V., Fujimoto, S., Labbe, I., et al. 2023, ApJL, 957, L7, doi: 10.3847/2041-8213/ad037a

Lovell, C. C., Harrison, I., Harikane, Y., Tacchella, S., & Wilkins, S. M. 2023, MNRAS, 518, 2511, doi: 10.1093/mnras/stac3224

Maiolino, R., Scholtz, J., Witstok, J., et al. 2024, Nature, 627, 59, doi: 10.1038/s41586-024-07052-5

Matthee, J., Naidu, R. P., Kotiwale, G., et al. 2025, ApJ, 988, 246, doi: 10.3847/1538-4357/ade886

Naidu, R. P., Oesch, P. A., van Dokkum, P., et al. 2022, ApJL, 940, L14, doi: 10.3847/2041-8213/ac9b22

Navarro-Carrera, R., Rinaldi, P., Caputi, K. I., et al. 2024, ApJ, 961, 207, doi: 10.3847/1538-4357/ad0df6

Pacucci, F., & Loeb, A. 2024, ApJ, 964, 154, doi: 10.3847/1538-4357/ad3044

Pezzulli, E., Valiante, R., & Schneider, R. 2016, MNRAS, 458, 3047, doi: 10.1093/mnras/stw505

Reines, A. E., & Volonteri, M. 2015, ApJ, 813, 82, doi: 10.1088/0004-637X/813/2/82

Schechter, P. 1976, ApJ, 203, 297, doi: 10.1086/154079

Silk, J., Begelman, M. C., Norman, C., Nusser, A., & Wyse, R. F. G. 2024, ApJL, 961, L39, doi: 10.3847/2041-8213/ad1bf0

Stone, M. A., Rieke, G. H., Lyu, J., et al. 2025, ApJ, 993, 168, doi: 10.3847/1538-4357/ae062a

Taylor, A. J., Finkelstein, S. L., Kocevski, D. D., et al. 2025, ApJ, 986, 165, doi: 10.3847/1538-4357/add15b

Weaver, J. R., Davidzon, I., Toft, S., et al. 2023, A&A, 677, A184, doi: 10.1051/0004-6361/202245581

Yue, M., Eilers, A.-C., Simcoe, R. A., et al. 2024, ApJ, 966, 176, doi: 10.3847/1538-4357/ad3914